

Design, Synthesis, Structural and Nonlinear Optical Properties of Photochromic Crystals: Toward Reversible Molecular Switches

Michel Sliwa,^{†,¶} Sylvie Létard,[†] Isabelle Malfant,[#] Martine Nierlich,[§] Pascal G. Lacroix,[#] Tsuyoshi Asahi,[¶] Hiroshi Masuhara,[¶] Pei Yu,^{*,‡} and Keitaro Nakatani^{*,†}

Laboratoire de Photophysique et de Photochimie Supramoléculaires et Macromoléculaires (PPSM, CNRS UMR 8531), Institut d'Alembert (IFR 121), Ecole Normale Supérieure de Cachan, 61 avenue du Président Wilson, 94235 Cachan Cedex, France, Laboratoire de Chimie Inorganique (LCI, CNRS UMR 8613), Université Paris-Sud, Bâtiment 420, 91405 Orsay Cedex, France, CEA Saclay, DRECAM/SCM, Bâtiment, 125, 91191 Gif-sur-Yvette Cedex, France, Laboratoire de Chimie de Coordination (LCC, CNRS UPR 8241), 205 route de Narbonne, 31077 Toulouse Cedex, France, and Department of Applied Physics, Handai Frontier Research Center, Graduate School of Engineering, Osaka University, Yamadaoka 2-1, Suita, Osaka 565-0871, Japan

Received May 3, 2005

Two new anil molecules exhibiting photochromism in the crystalline state, *N*-(4-hydroxy)-salicylidene-amino-4-(methylbenzoate) (**2**) and *N*-(3,5-di-*tert*-butylsalicylidene)-4-aminopyridine (**3**), are obtained. Upon irradiation in the UV, the yellow crystals change color to red, owing to enol-keto intramolecular tautomerism. The red color disappears, when crystals are left in the dark or irradiated with visible light. **3** has the most stable keto form among all anil-type photochromic compounds ($\tau = 460$ days at room temperature). Both exhibit nonlinear optical (NLO) properties and show powder second harmonic generation (SHG) of respectively 10 and 3 times vs urea. X-ray diffraction shows acentric structures where molecules line up "head-to-tail" through hydrogen bonds for **2** (space group *Pc*), or form a chiral helix **3** (space group *P3₂*). Evidence of reversible structural change is given for **3**, and we demonstrate the functionality of this crystal as an NLO switching material, as SHG can be photomodulated by about 30%.

Introduction

First observations of light-induced reversible color change date back to the end of the XIXth century.¹ This phenomenon, known as photochromism,² has been appealing to many research groups during the past century because not only color but also other properties such as refractive index, fluorescence, magnetic properties, electron transfer, or structural features can be reversibly modified.³ Applications as switches and sensors can be foreseen.⁴ Although based on light-induced excitation photochromism is not just a ground state to excited state transition, but a real chemical reaction between two molecules, large property changes are

detected. Light is a convenient way to trigger changes since it is widely available and can be transported rather easily without significant loss or interference, both in air or through materials such as fibers, thus enabling remote control.

Among all physical properties, our interest focused on second-order nonlinear optical (NLO) properties, and especially on second harmonic generation (SHG).⁵ In fact, light frequency conversion is an important issue, for instance, in

* To whom correspondence should be addressed. E-mail, nakatani@ppsm.ens-cachan.fr; tel., +33-1-4740-5338; fax, +33-1-4740-2454 (K. Nakatani). E-mail, yupe@icmo.u-psud.fr; tel., +33-1-6915-6183; fax, +33-1-6915-4754 (P. Yu).

[†] PPSM, CNRS UMR 8531, Ecole Normale Supérieure de Cachan.

[‡] LCI, CNRS UMR 8613, Université Paris-Sud.

[§] CEA Saclay, DRECAM/SCM.

[#] LCC, CNRS UPR 8241.

[¶] Osaka University.

- (1) (a) Fritzsche, M. *Compt. Rend.* **1867**, 169, 1035. (b) ter Meer, E. *Ann. Chem.* **1876**, 181, 122. (c) Marckwald, W. *Z. Phys. Chem.* **1899**, 30, 140.
- (2) (a) *Photochromism*; Brown, G. H., Ed.; Wiley-Interscience: New York, 1971. (b) *Photochromism: Molecules and Systems*; Dürr, H., Bouas-Laurent, H., Eds.; Elsevier: Amsterdam, The Netherlands, 1990. (c) *Organic Photochromic and Thermochromic Compounds*; Crano, J. C., Guglielmetti, R. J., Eds.; Plenum: New York, 1998. (d) Special Issue on Photochromism: Memories and Switches. *Chem. Rev.* **2000**, 100, issue 5. (e) Bouas-Laurent, H.; Dürr, H. *Pure Appl. Chem.* **2001**, 73, 639. (f) *Molecular Switches*; Feringa, B. L., Ed.; Wiley-VCH: Weinheim, Germany, 2001.

- (3) (a) Biteau, J.; Chaput, F.; Lahliou, K.; Boilot, J. P.; Tsivgoulis, G. M.; Lehn, J. M.; Darracq, B.; Marois, C.; Lévy, Y. *Chem. Mater.* **1998**, 10, 1945. (b) Kawai, T.; Fukuda, N.; Gröschl, D.; Kobatake, S.; Irie, M. *Jpn. J. Appl. Phys., Part 2* **1999**, 38, L1194. (c) Chauvin, J.; Kawai, T.; Irie, M. *Jpn. J. Appl. Phys., Part 1* **2001**, 40, 2518. (d) Norsten, T. B.; Branda, N. R. *J. Am. Chem. Soc.* **2001**, 123, 1784. (e) Fukaminato, T.; Kawai, T.; Kobatake, S.; Irie, M. *J. Phys. Chem. B* **2003**, 107, 8372. (f) Dvorkin, A.; Liang, Y.; Rentzepis, P. *J. Mater. Chem.* **2005**, 15, 1072. (g) Matsuda, K.; Irie, M. *Chem.-Eur. J.* **2001**, 7, 3466. (h) Matsuda, K.; Matsuo, M.; Mizoguti, S.; Higashiguchi, K.; Irie, M. *J. Phys. Chem. B* **2002**, 106, 11218. (i) Bénard, S.; Rivière, E.; Yu, P.; Nakatani, K.; Delouis, J. F. *Chem. Mater.* **2001**, 13, 159. (j) Kikuchi, A.; Iyoda, T.; Abe, J. *Chem. Commun.* **2002**, 1484. (k) Frayssé, S.; Coudret, C.; Launay, J. P. *Eur. J. Inorg. Chem.* **2000**, 1581. (l) Raymo, F. M.; Tomasulo, M. *Chem. Soc. Rev.* **2005**, 34, 327. (m) Irie, M.; Kobatake, S.; Horichi, M. *Science* **2001**, 291, 1769.
- (4) (a) Alfimov, M. V.; Fedorova, O. A.; Gromov, S. P. *J. Photochem. Photobiol. A* **2003**, 158, 183. (b) Kang, J. W.; Kim, J. J.; Kim, E. *Appl. Phys. Lett.* **2002**, 80, 8710. (c) Malval, J. P.; Gosse, I.; Morand, J. P.; Lapouyade, R. *J. Am. Chem. Soc.* **2002**, 124, 904.
- (5) (a) *Nonlinear Optical Properties of Organic Molecules and Crystals*; Zyss, J., Chemla, D. S., Eds.; Academic Press: Orlando, FL, 1987. (b) *Molecular Nonlinear Optics*; Zyss, J., Ed.; Academic Press: San Diego, CA, 1994. (c) Special Issue on Optical Nonlinearities in Chemistry. *Chem. Rev.* **1994**, 94, issue 1. (d) *Nonlinear Optics of Organic Molecules and Polymers*; Nalwa, H. S., Miyata, S., Eds.; CRC Press: Boca Raton, FL, 1996.

optical telecommunications. Although inorganic materials exhibiting such properties are commercially available, new molecular (especially organic and organometallic) materials are of increasing importance.⁶ These new materials compete well with more classical ones in term of intrinsic performance, but can also bring a high added value: they are easier to process and two or more different properties can be combined in one molecule.

During the past decade, an increasing number of research groups have been looking for switchable NLO systems.⁷ Targets are “push-pull” molecules exhibiting high quadratic hyperpolarizability (β), where properties could be largely modified by photochemical,⁸ electrochemical,⁹ or acido-basic reaction.¹⁰ Among them several examples of efficient molecules for photoswitching were reported,^{8a,b,e} and this principle was applied in a few cases to surface-deposited¹¹ materials. In a previous work we attempted to get higher SHG intensity by using “3D” bulk¹² materials. In fact, extending molecular properties to the material's scale is an actual challenge for the following reasons: SHG efficiency of a material is mostly related to the material's quadratic susceptibility ($\chi^{(2)}$), rather than β , and molecular materials arranged in a centrosymmetric fashion have no $\chi^{(2)}$, even if the molecules have high β ; most photochromic molecules lose this property in the solid state. Finally, penetration depth of light is another problem typical of photoresponsive bulk materials.

More generally, prediction of the crystal packing is an unsolved issue since it cannot be directly deduced from the molecular structure.¹³ In other words, the challenge is to

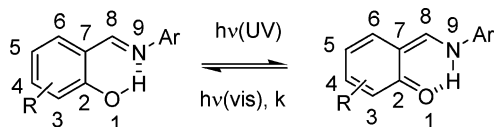
design molecules with NLO properties, which crystallize in a non-centrosymmetric space group and undergo photochromic reaction in the solid state.

For our first attempt to make photoswitchable NLO materials, we used poled poly(methyl methacrylate) (PMMA) polymers doped by “push-pull” photochromic molecules (azobenzene and furylfulgide).¹⁴ The poling process is aimed to break the centrosymmetry of molecular orientation in the polymer matrix. On poled thin films of these materials, a light-induced SHG change could be evidenced. However, the lifetime of these “switches” was short, and the reversibility of SHG change could only be guaranteed for a limited number of cycles since the photochemical reaction induced randomization of the molecules' orientation. As a consequence, despite the reversibility of the photochemical reaction, after a few cycles, $\chi^{(2)}$ went down to zero. To avoid this loss of non-centrosymmetry, permanent application of an electric field is necessary even after the poling process;¹⁵ thus, our interest turned to crystalline materials. Until the recent discovery of solid-state photochromism in some crystalline spiropyrans¹⁶ and diarylethenes,¹⁷ or under extreme conditions,¹⁸ photochromism in the crystalline state was rather scarce, despite the fact that photochemistry and bistability in the solid state are well-known phenomena.¹⁹ It could be encountered only in some families of compounds, such as salicylidene-anilines and related compounds,²⁰ benzylpyridines,²¹ or bisimidazoles,²² either by intramolecular tautomerism or homolytic bond cleavage.

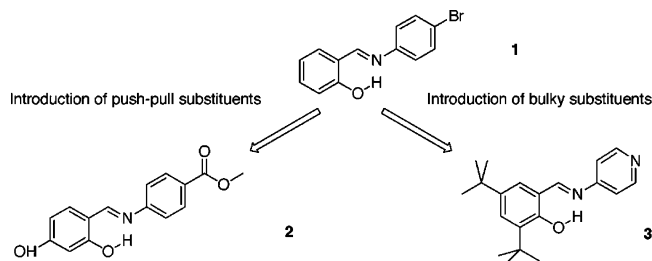
In salicylidene-anilines, salicylidene-aminopyridines, and related Schiff bases, generally called anils, an intramolecular proton transfer or tautomeric reaction between “—OH”, the enol(-imine) form, and “—NH”, the keto(-amine) form can occur both in solution and in the crystalline state (Scheme 1). This reaction can be induced either by light or by heat and is even encountered in biological media.²³ This feature leads to photochromic or thermochromic molecules and crystals. Although many references mention that thermo- and photochromism are mutually exclusive in anil crystals, a recent paper deals with a compound exhibiting both properties.²⁴ The initial “—OH” form is usually colorless or slightly

- (6) (a) Di Bella, S. *Chem. Soc. Rev.* **2001**, 30, 355. (b) Cho, M.; An, S. Y.; Lee, H.; Ledoux, I.; Zyss, J. *J. Chem. Phys.* **2002**, 116, 9165. (c) Klays, K.; Coe, B. J. *Chem. Mater.* **2003**, 15, 642. (d) Cifuentes, M. P.; Humphrey, M. G. *J. Organomet. Chem.* **2004**, 689, 3968. (e) Leclerc, N.; Sanaur, S.; Galmiche, L.; Mathevet, F.; Attias, A. J.; Fave, J. L.; Roussel, J.; Hapiot, P.; Lemaître, N.; Geffroy, B. *Chem. Mater.* **2005**, 17, 502.
- (7) (a) Coe, B. J. *Chem.-Eur. J.* **1999**, 5, 2464. (b) Asselberghs, I.; Clays, K.; Persoons, A.; Ward, M. D.; McCleverty, J. J. *Mater. Chem.* **2004**, 14, 2831.
- (8) (a) Gilat, S. L.; Kawai, S. H.; Lehn, J. M. *Chem.-Eur. J.* **1995**, 1, 275. (b) Houbrechts, S.; Clays, K.; Persoons, A.; Pikramenou, Z.; Lehn, J. M. *Chem. Phys. Lett.* **1996**, 258, 485. (c) Majumdar, D.; Lee, H. M.; Kim, J.; Kim, K. S.; Mhin, B. J. *J. Chem. Phys.* **1999**, 111, 5866. (d) Delaire, J. A.; Nakatani, K. In ref 2d, 1817. (e) Delaire, J. A.; Fanton-Maltes, I.; Chauvin, J.; Nakatani, K. *Mol. Cryst. Liq. Cryst.* **2000**, 345, 233.
- (9) (a) Coe, B. J.; Houbrechts, S.; Asselberghs, I.; Persoons, A. *Angew. Chem., Int. Ed.* **1999**, 38, 366. (b) Weyland, T.; Ledoux, I.; Brasselet, S.; Zyss, J.; Lapinte, C. *Organometallics* **2000**, 19, 5235. (c) Paul, F.; Costuas, K.; Ledoux, I.; Deveau, S.; Zyss, J.; Halet, J. F.; Lapinte, C. *Organometallics* **2002**, 21, 5229. (d) Asselberghs, I.; Clays, K.; Persoons, A.; McDonagh, A. M.; Ward, M. D.; McCleverty, J. *Chem. Phys. Lett.* **2003**, 368, 408.
- (10) (a) Hurst, S. K.; Cifuentes, M. P.; Morrall, J. P. L.; Lucas, N. T.; Whittall, I. R.; Humphrey, M. G.; Asselberghs, I.; Persoons, A.; Samoc, M.; Luther-Davies, B.; Willis, A. C. *Organometallics* **2001**, 20, 4664. (b) Asselberghs, I.; Zhao, Y.; Clays, K.; Persoons, A.; Comito, A.; Rubin, Y. *Chem. Phys. Lett.* **2002**, 364, 279.
- (11) (a) Meredith, G. R.; Krongauz, V.; Williams, D. J. *Chem. Phys. Lett.* **1982**, 87, 289. (b) Sakaguchi, H.; Gomez-Jahn, L. A.; Prichard, M.; Penner, T. L.; Whitten, D. G.; Nagamura, T. *J. Phys. Chem.* **1993**, 97, 1474. (c) Sato, O.; Baba, R.; Hashimoto, K.; Fujishima, A. *Denki Kagaku* **1994**, 62, 530. (d) Yamada, K.; Otsubo, H.; Yonemura, H.; Yamada, S.; Matsuo, T. *Chem. Lett.* **1997**, 451.
- (12) Nakatani, K.; Delaire, J. A. *Chem. Mater.* **1997**, 9, 2682.
- (13) (a) Gavazotti, A. *Acc. Chem. Res.* **1994**, 27, 309. (b) Curtin, D. Y. *Chem. Rev.* **1981**, 525. (c) Hulliger, J.; Bebie, H.; Kluge, S.; Quintel, A. *Chem. Mater.* **2002**, 14, 1523.

- (14) Atassi, Y.; Delaire, J. A.; Nakatani, K. *J. Phys. Chem.* **1995**, 99, 16320.
- (15) (a) Abe, J.; Hasegawa, M.; Matsushima, H.; Shirai, Y.; Nemoto, N.; Nagase, Y.; Takamiya, N. *Macromolecules* **1995**, 28, 2938. (b) Sekkat, Z.; Prêtre, P.; Knoesen, A.; Volksen, W.; Lee, V. Y.; Miller, R. D.; Wood, J.; Knoll, W. *J. Opt. Soc. Am. B* **1998**, 15, 401.
- (16) Benard, S.; Yu, P. *Chem. Commun.* **2000**, 65.
- (17) (a) Irie, M.; Uchida, K.; Eriguchi, T.; Tsuzuki, H. *Chem. Lett.* **1995**, 899. (b) Kobatake, S.; Shibata, K.; Uchida, K.; Irie, M. *J. Am. Chem. Soc.* **2000**, 122, 12135.
- (18) Asahi, T.; Suzuki, M.; Masuhara, H. *J. Phys. Chem. A* **2002**, 106, 2335.
- (19) (a) Ramamurthy, V. *Chem. Rev.* **1987**, 87, 3. (b) Tomlinson, W. J.; Chandross, E. A. In *Advances in photochemistry*; Pitt, J. N., Hammond, G. S., Gollnick, K., Eds.; Wiley-Interscience: New York, 1979; Vol. 12.
- (20) (a) Hadjoudis, E. In ref 2b, 685. (b) Senier, A.; Shepherd, F. G. *J. Chem. Soc.* **1909**, 95, 1943. (c) Senier, A.; Shepherd, F. G.; Clarke, R. *J. Chem. Soc.* **1912**, 101, 1952. (d) Hadjoudis, E. *Mol. Eng.* **1995**, 5, 301. (e) Hadjoudis, E.; Vittorakis, M.; Moustakali-Mavridis, I. *Tetrahedron* **1987**, 43, 1345. (f) Hadjoudis, E.; Mavridis, I. *Chem. Soc. Rev.* **2004**, 33, 579.
- (21) Tschitschibabin, A. E.; Kuindshi, B. M.; Benewolenskaja, S. W. *Ber. Dtsch. Chem. Ges.* **1925**, 58, 1580.
- (22) Hayashi, T.; Maeda, K. *Bull. Chem. Soc. Jpn.* **1960**, 33, 565.
- (23) Abou-Zied, O. K.; Jimenez, R.; Romesberg, F. E. *J. Am. Chem. Soc.* **2001**, 123, 4613.
- (24) Fujiwara, T.; Harada, J.; Ogawa, K. *J. Phys. Chem. B* **2004**, 108, 4035.

Scheme 1. Photochromism of Anils between the “–OH” Enol(imine) and the “–NH” Keto(amine) Form^a

^a In our case, Ar is a substituted phenyl or a pyridine group.

Scheme 2. Anil Molecules Designed for Solid State NLO Photoswitching

yellow with an absorption band in the near UV. The “–NH” form is usually red and exhibits an additional absorption band around 500 nm. Despite some exceptions,²⁵ the “–OH” form is usually the more stable one. Photochromic anils belong to the “T-type” ones since the back reaction from “–NH” to “–OH” form takes place both in the dark by thermal conversion and by irradiation with visible light.

NLO properties of some anils have been studied both on molecular and solid-state levels.²⁶ Compounds reported so far exhibit at best a powder SHG intensity equal to urea, except one (6.4 vs urea for *N*-salicylidene-2-chloro-4-nitroaniline),^{26b} and their β values range between 5 and 14×10^{-30} esu.^{26c} Although the authors mention the photo- or thermochromism of anils in the crystalline phase, none of them took advantage of this property to consider them as potential NLO switches.

N-Salicylidene-4-bromoaniline (**1**, Scheme 2) and some other anils are known to crystallize in non-centrosymmetric space groups and to exhibit photochromism in the crystalline state.^{27,28} They fulfill our requirements. We reported on SHG properties of these compounds²⁹ and the possibility to photoswitch this property for **1**.¹² UV irradiation of a polycrystalline powder of **1** induced a 10% decrease of the SHG intensity at 1907 nm. The initial SHG intensity was recovered either by visible irradiation or by leaving the sample in the dark at room temperature. Since then, our aim was to improve the targeted properties and its modulation

by creating original molecules (Scheme 2), through the following strategies:

- (i) increase of the hyperpolarizability β , by introduction of “push-pull” substituents;
- (ii) stabilization of the “–NH” form, by introduction of bulky substituents, to have thermally stable switches.

According to the application, either “T-type” photochromes with fast thermal back reaction (ophthalmic application) or “P-type” photochromes with infinitely slow thermal back reaction (optical memories) are suitable. The kinetics of this back reaction is an important parameter. Finally, from a fundamental point of view, we expect that slowing down this reaction would make easier the structural and spectroscopic investigations of the metastable “–NH” form.

This paper focuses on two original compounds, *N*-(4-hydroxy)-salicylidene-amino-4-(methylbenzoate) (**2**) and *N*-(3,5-di-*tert*-butylsalicylidene)-4-aminopyridine (**3**) (Scheme 2). The well-known “push-pull” scheme for second-order NLO was directly applied in the design of **2** by the introduction of hydroxy and ester groups on para positions at both ends of the basic anil structure. In **3**, we introduced bulky *tert*-butyl groups. The influence of bulky substituents on either six-membered ring was thoroughly studied by T. Kawato et al. and led to the conclusion that the “–NH” isomer is stabilized when such substituents are introduced.³⁰

Both **2** and **3** are photochromic in the solid state and crystallize in non-centrosymmetric space groups. We report and discuss on spectroscopic, photochemical, and NLO properties of **2** and **3** and correlate with structures determined by X-ray diffraction and with theoretical calculations. Finally, we evidenced photoswitching of NLO properties in crystals of **3**, along with structural changes.

Experimental Section

Synthesis. All reagents (Aldrich) and solvents (SDS) were used as received, without any further purification. Elemental analysis was made by the Service de Microanalyse du CNRS (Gif sur Yvette and Vernaison). ¹H NMR were recorded on a Bruker 300 MHz NMR and FTIR spectra on a Thermo-Optek Nexus.

Compound 2. Equimolar amounts of 2,4-dihydroxybenzaldehyde (1.4 g) and 4-amino-methylbenzoate (1.5 g) were dissolved in 40 mL of methanol. The mixture was stirred under reflux for 1 h, and cooling to room temperature yielded yellow crystals. The crystals of **2** were isolated by filtration (1.3 g, 50%). Recrystallization in methanol: mp (dec) 180 °C. Anal. Calcd for C₁₅H₁₃NO₄: C, 66.41%; H, 4.83%; N, 5.16%; O, 23.59%. Found: C, 66.21%; H, 4.67%; N, 5.19%; O, 23.45%. ¹H NMR (DMSO, 300 MHz): δ 3.89 (s, 3H), 6.35 (d, 1H, J 2.2 Hz), 6.46 (dd, 1H, J 2.2 Hz), 7.48 (d, 2H, J 8.4 Hz), 7.51 (d, 1H, J 8.5 Hz), 8.04 (d, 2H, J 8.4 Hz), 8.89 (s, 1H), 10.43 (s, 1H), 13.21 (s, 1H). IR: 1630 cm⁻¹ (medium, C=N), 1576 cm⁻¹ (strong, aromatic), 1514 cm⁻¹ (medium, aromatic).

Compound 3. **3** was obtained by the condensation of equimolar amounts of 3,5-di-*tert*-butylsalicylaldehyde (2.3 g) and 4-aminopyridine (0.94 g). Since the usual procedure in methanol or ethanol solution gave low yields (<10%), the reaction was performed by

- (25) (a) Kabak, M.; Elmali, A.; Elerman, Y. *J. Mol. Struct.* **1999**, 477, 151. (b) Ogawa, K.; Harada, J.; Tamura, I.; Noda, Y. *Chem. Lett.* **2000**, 528. (c) Chong, J. H.; Sauer, M.; Patrick, B. O.; MacLachlan, M. J. *Org. Lett.* **2003**, 5, 3823.
- (26) (a) Palazzotto, M. C. Minnesota Mining and Manufacturing Company, U.S. Patent 4,733,109, 22 March 1988. (b) Bhat, K.; Chang, K. J.; Aggarwal, M. D.; Wang, W. S.; Penn, B. G.; Frazier, D. O. *Mater. Chem. Phys.* **1996**, 44, 261. (c) Zhang, Y.; Zhao, C. Y.; Fang, W. H.; You, X. Z. *Theor. Chem. Acc.* **1997**, 96, 129.
- (27) Cohen, M. D.; Schmidt, G. M. J.; Flavian, S. *J. Chem. Soc.* **1964**, 2041.
- (28) Lindeman, S. V.; Shklover, V. E.; Struchkov, Yu. T.; Kravcheny, S. G.; Potapov, V. M. *Cryst. Struct. Commun.* **1982**, 11, 49.
- (29) Poineau, F.; Nakatani, K.; Delaire, J. A. *Mol. Cryst. Liq. Cryst.* **2000**, 344, 89.

- (30) (a) Kawato, T.; Koyama, H.; Kanatomi, H.; Isshiki, M. *J. Photochem.* **1985**, 28, 103. (b) Kawato, T.; Koyama, H.; Kanatomi, H.; Tagawa, H.; Iga, K. *J. Photochem. Photobiol. A* **1994**, 78, 71.

melting the aldehyde (mp 60 °C) and dissolving the amine in the liquid aldehyde. After 2 h of stirring under reflux at 140 °C, the mixture turned red and crystals appeared. Diethyl ether was added to the mixture, and the target compound precipitated as yellow crystals. The crystals were isolated by filtration (1.9 g, 60%) and recrystallized in diethyl ether. mp 190 °C. Anal. Calcd for $C_{20}H_{26}N_2O$: C, 77.38%; H, 8.44%; N, 9.02%; O, 5.15%. Found: C, 77.31%; H, 8.43%; N, 8.87%; O, 4.89%. 1H NMR (DMSO, 300 MHz): δ 1.34 (s, 9H), 1.46 (s, 9H), 7.45 (d, 2H, J 5.1 Hz), 7.50 (d, 1H, J 2.2 Hz), 7.58 (d, 1H, J 2.2 Hz), 8.66 (d, 2H, J 5.1 Hz), 9.00 (s, 1H), 13.49 (s, 1H). IR: 1616 cm^{-1} (medium, C=N), 1576 cm^{-1} (strong, aromatic).

Sample Preparation. Single crystals for X-ray diffraction were obtained by slow evaporation of a methanol solution for **2** and of an acetone/petroleum ether solution for **3**. Crystallinity was checked under a polarized light microscope.

Polycrystalline thin films for spectroscopic and NLO measurements of **3** were made by melting crystalline powder between two microscope glass blades (1/10 mm). Thickness was estimated to be around 10 μm , from weight and density values. In the case of **2**, since decomposition occurs instead of melting, thin films were made by vacuum vapor deposition (6×10^{-4} mbar, 200 °C).

X-ray Diffraction. *Compound 2.* Data were collected at low temperature on a IPDS STOE diffractometer using a graphite-monochromated Mo K α radiation ($\lambda = 0.71073$ Å) and equipped with an Oxford Cryosystems Cryostream Cooler Device. The final unit cell parameters have been obtained by means of a least-squares refinement performed on a set of 5000 well-measured reflections, and a crystal decay has been monitored during the data collections; no significant fluctuations of intensities have been observed. The structures have been solved by Direct Methods using SIR92³¹ and refined by means of least-squares procedures on a F^2 with the aid of the program SHELXL97³² included in the software package WinGX version 1.63.³³ The Atomic Scattering Factors were taken from International Tables for X-Ray Crystallography.³⁴ All hydrogens atoms were located on a difference Fourier map and refined by using a riding model.

All non-hydrogens atoms were anisotropically refined, and in the last cycles of refinement a weighting scheme was used, where weights are calculated from the following formula: $w = 1/[\sigma^2(F_o^2) + (aP)^2 + bP]$ where $P = (F_o^2 + 2F_c^2)/3$.

Drawing of molecules is performed with the program ORTEP32³⁵ with 50% probability displacement ellipsoids for non-hydrogen atoms.

Compound 3. Diffraction collection was carried out on a Nonius diffractometer (Mo K α , $\lambda = 0.71073$ Å) equipped with a CCD detector. The lattice parameters were determined from 10 images recorded with 2° Φ -scans and later refined on all data. The data were recorded at 173 K. A 180° Φ -range was scanned with 2° steps with a crystal to detector distance fixed at 30 mm. Data were corrected for Lorentz-polarization. The structure was solved by the direct methods (SHELXS-97)³² and refined by full-matrix least-squares on F^2 with anisotropic thermal parameters for all non-H atoms. H atoms (except H of OH group) were introduced at calculated positions and constrained to ride on their parent C atom.

The H atom of OH, found in the last Fourier difference, was not refined but introduced at fixed positions. The Flack parameter is $-1(3)$ in $P3_2$ and $1(3)$ in $P3_1$; the absolute structure cannot be determined reliably.

All calculations were performed on an O2 Silicon Graphics Station with the SHELXTL package.³²

Compound 3 Measurements under Irradiation. Data were collected at low temperature on a Xcalibur Oxford Diffraction diffractometer using a graphite-monochromated Mo K α radiation ($\lambda = 0.71073$ Å) and equipped with an Oxford Cryosystems Cryostream Cooler Device. The final unit cell parameters have been obtained by means of a least-squares refinement performed on a set of 5000 well-measured reflections, and a crystal decay has been monitored during the data collections; no significant fluctuations of intensities have been observed.

Dipole Moments and SHG Measurements. Measurements were mainly performed at 1907 nm. This wavelength was generated by focusing the 1064 nm fundamental beam of a nanosecond Nd:YAG pulsed laser in a Raman-shifting hydrogen cell (40 bar, 1 m long) and used as the fundamental beam for SHG measurements. The SHG intensity was detected by a photomultiplier (Hamamatsu) and the signal was read on an oscilloscope (Tektronic TDS 620). For electric field induced second harmonics (EFISH) technique,³⁶ the centrosymmetry of the solution was broken by applying a pulsed electric field of 5 kV for 5 μs (Lasermetrics). Solutions of MNA (2-methyl-4-nitroaniline, $\mu\beta = 71 \times 10^{-48}$ esu at 1907 nm) served as reference. For powder tests, SHG intensities were compared to urea powder. Dielectric constant and diffractive index were measured respectively by a dipole-meter (WTW) and an Abbe Refractometer (Carl Zeiss), and the data were analyzed following the Guggenheim's method.³⁷

To generate other fundamental wavelengths, the output from a Ti:sapphire laser (with a regenerative amplifier, 780 nm, 3–4 mJ-pulse⁻¹, 170 fs fwhm, 10 Hz) was focused into a 1 cm quartz cell containing H₂O. The outcoming continuum was filtered (silicon plate), focused in a confocal microscope, and used as the fundamental beam for SHG measurements between 0.9 and 1.4 μm .

UV–Visible Spectra. UV–visible absorption spectra were recorded on a Varian Cary 5, for solution and polycrystalline thin film measurements. Spectra in solution were recorded vs blank solvent (spectrophotometric grade). Data on single crystals (Figure 8) were recorded under a confocal microscope.

Photochromic Properties (Experiments under Irradiation). A Hg–Xe UV–visible Hamamatsu (LC6 Lightningcure, 150 W) lamp equipped with an optical fiber was used to induce the photochromic reaction. Appropriate wavelengths were chosen by interposing appropriate band-pass or interference filters. Samples were irradiated by this source in situ within the diffractometer, the SHG setup, the spectrophotometer, or the confocal microscope.

Theoretical Calculations. The all-valence INDO (intermediate neglect of differential overlap) formalism,³⁸ in connection with the sum over state (SOS) formalism, was employed for the calculation of the electronic spectra and the molecular hyperpolarizabilities.³⁹ In the present approach, the mono-excited configuration interaction

(31) Altomare, A.; Casciaro, G.; Giacovazzo, C.; Guagliardi, A. *J. Appl. Crystallogr.* **1993**, 26, 343.

(32) Sheldrick, G. M. *SHELX97* [Includes SHELXS97, SHELXL97, CIFTAB]—Programs for Crystal Structure Analysis (Release 97-2); Institut für Anorganische Chemie der Universität: Göttingen, Germany, 1998.

(33) Farrugia, J. L. *J. Appl. Crystallogr.* **1999**, 32, 837.

(34) *International Tables for X-Ray Crystallography*; Kynoch Press: Birmingham, U.K., 1974; Vol. IV.

(35) Farrugia, J. L. *J. Appl. Crystallogr.* **1997**, 30, 565.

(36) (a) Bosshard, C.; Knöpfle, G.; Prêtre, P.; Günter, P. *J. Appl. Phys.* **1992**, 71, 1594. (b) Maltey, I.; Delaire, J. A.; Nakatani, K.; Wang, P.; Shi, X.; Wu, S. *Adv. Mater. Opt. Electron.* **1996**, 6, 233. (c) Liu, C. S.; Glaser, R.; Sharp, P.; Kauffmann, J. F. *J. Phys. Chem. A* **1997**, 101, 7176.

(37) (a) Guggenheim, E. A. *Trans. Faraday Soc.* **1949**, 714. (b) Janini, G. M.; Katrib, A. H. *J. Chem. Educ.* **1983**, 60, 1087. (c) Chen, G. S.; Liu, C. S.; Glaser, R.; Kauffmann, J. F. *Chem. Commun.* **1996**, 1719.

(38) (a) Zerner, M.; Loew, G.; Kirchner, R.; Mueller-Westerhoff, U. J. *Am. Chem. Soc.* **1980**, 102, 589. (b) Anderson, W. P.; Edwards, D.; Zerner, M. C. *Inorg. Chem.* **1986**, 25, 2728.

(39) Ward, J. F. *Rev. Mod. Phys.* **1965**, 37, 1.

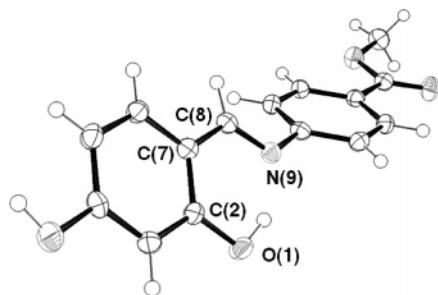


Figure 1. ORTEP drawing of **2**, showing 50% probability displacement ellipsoids. The orientation of the molecule in the crystal lattice is represented in Figure 5.

Table 1. Crystal Data and Structure Refinement of 2 and 3

	2	3
formula	C ₁₅ H ₁₃ NO ₄	C ₂₀ H ₂₆ N ₂ O
formula weight	271.26	310.43
$\lambda/\text{\AA}$	0.71073 (Mo K α)	0.71073 (Mo K α)
temperature/K	180	173(2)
crystal system	monoclinic	trigonal
space group	Pc	P3 ₂
$a/\text{\AA}$	14.739(2)	16.002(2)
$b/\text{\AA}$	7.027(1)	16.002(2)
$c/\text{\AA}$	6.096(1)	6.040(1)
α/deg	90	90
β/deg	99.21(1)	90
γ/deg	90	120
$V/\text{\AA}^3$	623.2(1)	1339.4(4)
Z	2	3
$\rho_{\text{calc}}/\text{g cm}^{-3}$	1.446	1.155
μ/mm^{-1}	0.106	0.071
$F(000)$	284	504
θ range/deg	2.65/26.05	2.94/24.70
reflections collected	5732	8397
independent reflections	1211	2840
no. of restraints/parameters	2/189	1/209
goodness-of-fit on F^2	1.097	1.016
R1 ($I > 2\sigma(I)$)	0.0288	0.0544
wR2 (all data)	0.0768	0.120
largest diff. peak/hole [$e \cdot \text{\AA}^{-3}$]	0.172/−0.162	0.193/−0.176

(CIS) approximation was employed to describe the excited states. The lowest 100 energy transitions were chosen to undergo CI mixing. All calculations were performed using the INDO/1 Hamiltonian incorporated in the commercially available software package ZINDO.⁴⁰

Results and Discussion

X-ray Crystallographic Structure of 2 and 3. Crystallographic structures of **2** and **3** were determined by X-ray diffraction (Table 1) and the ORTEP views are shown in Figures 1 and 2. The two compounds share some common characteristics. First of all, in both crystals, the molecules are in the “−OH” form. Distances between the atoms O¹—C²—C⁷—C⁸—N⁹ (numbering is explained in Scheme 1) are compatible with the enol-imine structure (Table 2). The “−OH”/“−NH” switching is possible due to the hydrogen bond between the enol hydrogen atom and the imine nitrogen atom: 1.68(3) Å for **2** and 1.77 Å for **3**. Finally, contrary to thermochromic compounds where the anil structure is almost planar, **2** and **3** show the typical distortion of photochromic anils: the mean planes of the six-membered rings make an angle of respectively 47.69(4)° and 41.8(1)°.

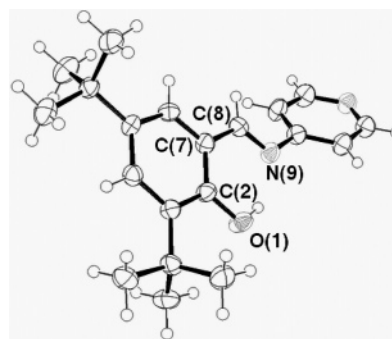


Figure 2. ORTEP drawing of **3**, showing 50% probability displacement ellipsoids. The orientation of the molecule in the crystal lattice is represented in Figure 4.

Table 2. Main Intramolecular Structural Characteristics of 2 and 3

	interatomic distances ^a /Å				$d(\text{N}\cdots\text{H})^b/\text{\AA}$	distortion angle ^c /°
	O ¹ —C ²	C ² —C ⁷	C ⁷ —C ⁸	C ⁸ —N ⁹		
2	1.350(2)	1.419(2)	1.439(3)	1.290(2)	1.68(3)	47.69(4)
3	1.354(4)	1.417(5)	1.448(5)	1.281(4)	1.77	41.8(1)

^a Atom numbering as defined in Scheme 1. ^b Distance between the enol hydrogen and the imine nitrogen atoms. ^c Angle between the mean planes of the six-membered rings.

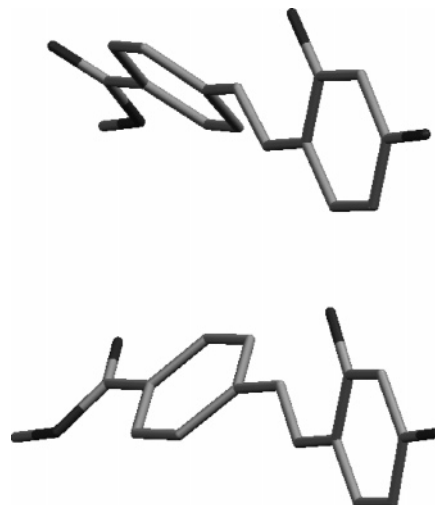


Figure 3. Molecules' configuration in the crystal of **2**. In the case of **2**, the two configurations exist within the same single crystal, whereas in the case of **3**, only one configuration exists (Figures 2 and 4). Hydrogen atoms are omitted.

This structural distortion at the molecular scale has important consequences on the crystalline structure and eventually on the material's properties since it introduces “chirality” in the solid crystal: Figure 3 is a schematic view of **2** which shows that the above-mentioned distortion angle can be clockwise or counterclockwise. According to the X-ray structure, all molecules in the unit cell have the same distortion angle sign in **3** (Figures 2 and 4), and this leads inevitably to a non-centrosymmetric packing, which is a favorable situation for NLO properties. Molecules in the crystal are deduced from one another by a rotation of 120° around the c axis and a translation of one-third of a unit cell along the same axis. Hence, the molecules form helices around the c axis and the space group is $P3_2$.

The case of **2** (space group Pc) is somehow different: each unit cell is constituted of two molecules, and atomic coordinates of one molecule are deduced from the other one

(40) ZINDO, release 96.0; Molecular Simulations Inc.: Cambridge, U.K., 1996.

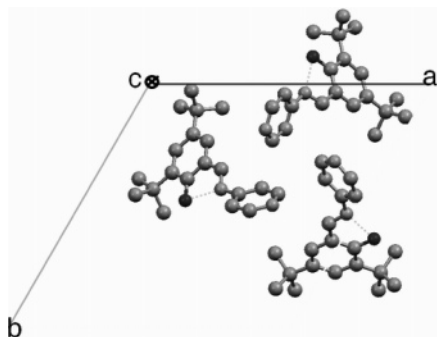


Figure 4. Unit cell of **3**, view along the *c* axis. The molecules have a helicoidal arrangement around the *c* axis. Hydrogen atoms are omitted.

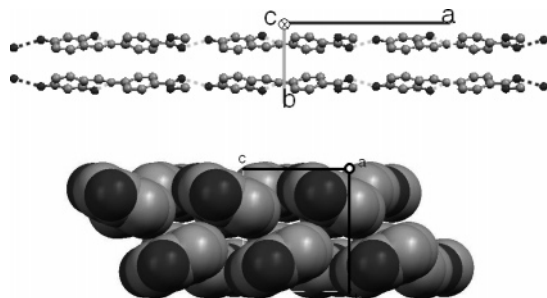


Figure 5. Unit cell of **2**, (a) view along the *c* axis showing the “head-to-tail” alignment of the molecules linked by intermolecular hydrogen bond between hydroxy and ester groups, (b) view along the *a* axis showing the van der Waals radius of the atoms and the close packing of the molecules. Hydrogen atoms are omitted.

by the symmetry operation $(X, Y, Z) \rightarrow (X, -Y, \frac{1}{2} + Z)$. This means that although the two molecules have “opposite” distortions angles in the unit cell (Figures 3 and 5) and form a “racemic” mixture, they align in a non-centrosymmetric fashion. The crystal system is monoclinic, but with all angles equal or close to 90° ($\beta = 99.21(1)^\circ$). The molecules are aligned head-to-tail, along the charge transfer axis, roughly parallel to the *a* axis. Along this axis, the molecules form a “chain”, linked by hydrogen bonds between the carbonyl oxygen and the enol hydrogen of the neighbor molecule: $O \cdots H$ distance, $1.94(3)$ Å, $O \cdots H-O$ angle, $158(3)^\circ$. Along the other directions, although no clear interaction such as π -stacking was evidenced, molecules are very tightly packed. As a consequence, the density of the solid is 1.446 for **2**, which is among the three highest values known for anils without heavy atoms.⁴¹ Moreover, **2** probably has a high melting point and decomposes at 180°C instead of melting.

Consequences of the structure on the NLO and photochemical properties for both molecules will be discussed in the following sections.

Molecular and Bulk NLO Properties: Experiments and Theoretical Calculations. By electric field induced second harmonics (EFISH) experiments,³⁶ we obtained values of $\beta \cdot \mu$, the scalar product of the quadratic hyperpolarizability, and the dipole moment (eq 1). The experiments were performed in dioxane, and the fundamental wavelength was 1907 nm (see Experimental Section for details). β_i , the components of β involved in this scalar product, are defined from the tensor elements β_{ijk} as written in eq 2. Dipole moments were also measured according to Guggenheim's

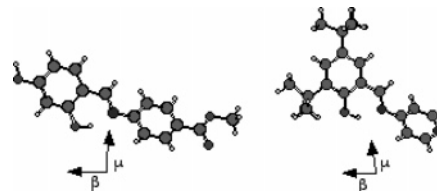


Figure 6. Representation of **2** (left) and **3** (right) in the (β, μ) plane with respective μ and β vector directions.

Table 3. Experimental and ZINDO Calculated Dipole Moments (μ in D) and Hyperpolarizabilities (β in 10^{-30} esu) at 1907 nm, for Compounds **1, **2**, and **3****

	$\beta\mu$ (exp.)	μ (exp.)	$\beta\mu$ (exp.)	$\beta\mu$ (th.)	μ (th.)	$\beta\mu$ (th.)	β (th.)	$\mu\beta$ angle $^\circ$
1	15.2	2.5	6.1	7.77	4.83	1.61	2.20	137.1
2	18.4	3.0	6.1	18.10	8.15	2.22	8.21	92.7
3	9.1	2.7	3.4	3.72	5.16	0.72	3.46	78.0

Table 4. Bulk NLO Properties: Powder Test and Theoretical Calculations

compound	1	2	3
powder test/urea	2.2 ^a	10	3
$B/10^{-30}$ esu	2.4	6.8	2.6
major B_{ijk} components	<i>ccc</i>	<i>caa</i> ^b	<i>aaa</i>
$/10^{-30}$ esu	1.2	1.0	6.8
		<i>Zaa</i> ^{b,c}	<i>ccc</i>
		3.3	1.6
			<i>caa</i> ^{b,d}
			0.5

^a Reference 29. ^b Other components, obtained by index rotation, have approximately the same value (Kleinman's theory).⁴⁵ ^c *Z* is perpendicular to the (*a*, *b*) plane. ^d For symmetry reasons, *caa* and *cbb* components have the same value.

method.³⁷ From these experimental data, the projection of the hyperpolarizability on the dipole moment direction (β_μ , eq 3) is deduced.

$$\beta \cdot \mu = \beta_x \mu_x + \beta_y \mu_y + \beta_z \mu_z \quad (1)$$

$$\beta_i = \beta_{iii} + \frac{1}{3} \sum_{j \neq i} (\beta_{ijj} + \beta_{jij} + \beta_{jji}) \quad (2)$$

$$\beta_\mu = \frac{\beta \cdot \mu}{||\mu||} \quad (3)$$

The $\beta \cdot \mu$ values are rather low and in the same order of magnitude as the previously reported compound **1** (Table 3). A rationale can be found from the examination of the calculations. According to these, β and μ are almost perpendicular, 92.7° for **2** and 78.0° for **3** (Figure 6). In both cases, as expected, β is almost along the major axis of the molecule since NLO properties are usually related to the charge-transfer ability of the molecule. μ seems to be strongly influenced by the intramolecular hydrogen bond, which apparently creates important charge densities on the atoms of the pseudo-six-membered ring $O_1-C_2-C_7-C_8-N_9-H$. Both experimental and theoretical values give $2 > 1 > 3$ for $\beta \cdot \mu$ and $2 > 3 > 1$ for μ . However, a discrepancy on the absolute value is clear and can be explained by the difference in environment and geometry between solution and gas phase,⁴² the experimental errors arising from EFISH experiments when $\beta \cdot \mu$ values are lower than 10^{-29} esu D.

Both **2** and **3** exhibit powder SHG (Table 4), with an intensity of respectively 10 and 3 times vs urea powder.

(41) Cambridge database <http://www.ccdc.cam.ac.uk>.

(42) Di Bella, S.; Marks, T. J.; Ratner, M. A. *J. Am. Chem. Soc.* **1994**, *116*, 4440.

Table 5. Maximum Absorption Wavelengths of 2 and 3 in Solution and in the Solid State

	2	3
cyclohexane	348;290	361;284
toluene	351;297	361;287
chloroform	349;295	362;289
methanol	348;293	362;290
acetonitrile	346;295	356;286
dimethyl sulfoxide	355;300	358;290
crystal ^a	355;290	368;292

^a Measured by reflection on microcrystalline powder with Kubelka–Munk analysis.⁴⁶

Among anils, **2** has the highest bulk SHG value reported so far.^{26b,c,29} This is due to the favorable packing of the molecules in the crystal. In fact, a bulk material has a non-zero $\chi^{(2)}$ and exhibits SHG, only if the molecules are favorably oriented. The components of the $\chi^{(2)}$ tensor ($\chi_{IJK}^{(2)}$) are connected to the components of β (β_{ijk}) by eqs 4 and 5.⁴³

$$\chi_{IJK}^{(2)} = NKB_{IJK} \quad (4)$$

$$B_{IJK} = -\sum_{n=1}^n \cos(I, i(s)) \cos(J, j(s)) \cos(K, k(s)) \beta_{ijk} \quad (5)$$

N is the number of molecules per crystal unit volume, n the number of molecules in the unit cell, and K a correction term including local field factors. Components of B (B_{IJK}) correspond to the NLO properties of an unit cell and are directly proportional to $\chi^{(2)}$. ZINDO calculations were performed on the unit cell considered as a whole.⁴⁴ The most significant components of B are mentioned in Table 4. For **2**, the two most important components are B_{aaa} and B_{Zaa} (Z is perpendicular to crystallographic axes a and b and almost parallel to c), which was logically foreseen since molecules line up along the a axis and lie almost in the Za plane. The situation is similar for **1** (orthorhombic, space group $Pca2_1$), where the molecules are globally lying in the ac plane and lining up along the c axis. Analogous calculations show that, for **3**, B_{ccc} along the axis of the helix is the highest component. Powder test SHG intensities increase with B_{IJK} values.

Spectroscopic Properties and Photochromism. **2** and **3** exhibit the usual absorption bands of anils in the UV. Both compounds show very little solvatochromism, and absorption bands in the solid state do not differ much from those in solution (Table 5). According to ZINDO calculations, mainly HOMO–LUMO and NHOMO–LUMO transitions contribute to these bands.

In solution, as for other anils,⁴⁷ the photochromic properties of **2** and **3** can be evidenced only by transient spectroscopy since the lifetime of the “–NH” form is of millisecond order.⁴⁶ UV irradiation of polycrystalline powder and thin film, as well as single crystals, induces the appearance of a

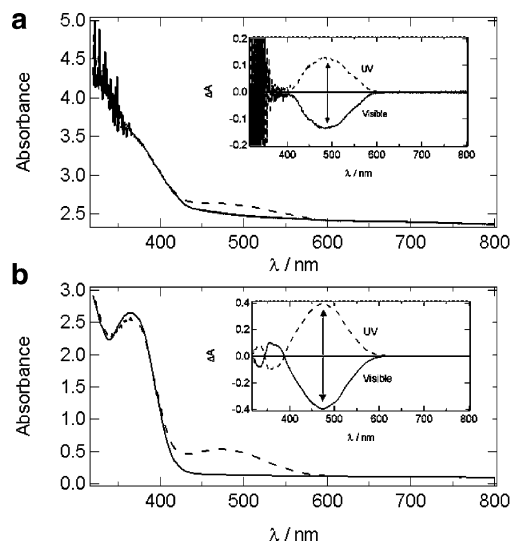


Figure 7. Transmission UV–visible absorption spectra of **2** (a) and **3** (b) polycrystalline thin films on glass. The solid line is the initial spectrum and the dashed line is the spectrum after UV irradiation. Insert shows evolution of spectra under UV irradiation and under consecutive visible irradiation.

red color, attributed to the “–NH” compound. Absorbance of the UV band decreases, and a new band appears in the visible (500 nm for **2** and 475 nm for **3**). The red color is rather weak for **2**, probably due to the close packing of the crystal which hinders the formation of “–NH” form. A photostationary state is reached after 30 min of irradiation at 365 nm (3 mW cm^{−2}). The reaction is far from being total. From the decrease of the absorbance of the UV band, the conversion is estimated to be at least 5% for **3** (Figure 7). Hence, although more than 90% of the 365 nm beam is absorbed by the first half of the sample, conversion not only is a surface effect but also occurs in part of the bulk (see also “Structural Change and SHG Commutation”). The conversion yield of **2** is so low that no quantitative determination was done. The initial absorption spectrum is recovered, after irradiation with visible light. This UV–visible cycle can be repeated several times, and both anils exhibit good fatigue resistance: after 40 cycles, the absorbance in the visible reached during UV irradiation has the same value (Figure 8).

After UV irradiation, the initial state can also be recovered through thermal reaction by leaving the polycrystalline thin film in the dark. Both for **2** and **3**, the kinetics of this reaction was fitted properly by a double exponential equation (Figure 9 and Table 6). This is rather usual for anils and is explained by a two-stage decay process of the “–NH” isomer.^{27,30a} For both compounds, the slower constant is the more important one. As expected, the *tert*-butyl bearing compound has a very slow back reaction. Moreover, with a kinetic constant of $1.8 \times 10^{-8} \text{ s}^{-1}$ at room temperature, **3** has the slowest decay known for anils, about 10 times slower than the record holder, *N*-(3,5-di-*tert*-butylsalicylidene)-3-nitroaniline ($k = 2.0 \times 10^{-7} \text{ s}^{-1}$).^{30a} It means that the half-life of the metastable “–NH” species is 460 days.

Heating samples of **2** and **3** speeds up the thermal back reaction.³⁰ The kinetic constant of the slower (and major) component was determined at different temperatures, and temperature dependence follows an Arrhenius law. The

(43) Zyss, J.; Oudar, J. L. *Phys. Rev. A* **1982**, 26, 2028.

(44) Zhu, X. L.; You, X. Z.; Zhong, Y.; Yu, Z.; Guo, S. L. *Chem. Phys.* **2000**, 253, 241.

(45) Kleinman, D. A. *Phys. Rev.* **1962**, 126, 1977.

(46) Sliwa, M.; Nakatani, K.; Asahi, T.; Masuhara, H. *Mol. Cryst. Liq. Cryst.* **2005**, 431, 241.

(47) (a) Nakagaki, R.; Kobayashi, T.; Nakamura, J.; Nagakura, S. *Bull. Chem. Soc. Jpn.* **1977**, 50, 1909. (b) Ohshima, A.; Momotake, A.; Arai, T. *J. Photochem. Photobiol. A* **2003**, 162, 473.

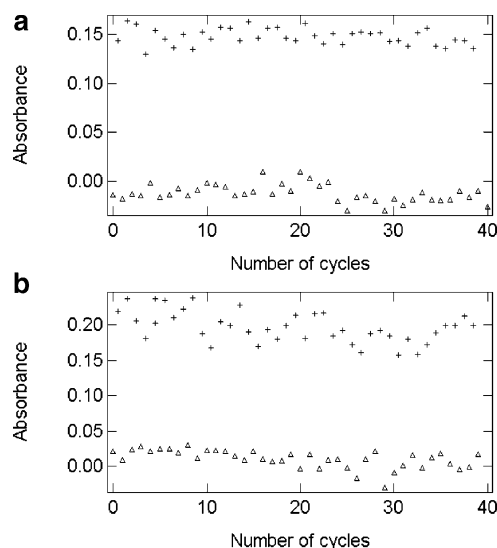


Figure 8. UV–visible cycles and fatigue resistance experiment on a single crystal. Absorbance at 500 nm for **2** (a) and **3** (b) after UV irradiation (cross) and consecutive visible irradiation (triangle). UV: 2 min, 405 nm; visible: 2 min, 532 nm.

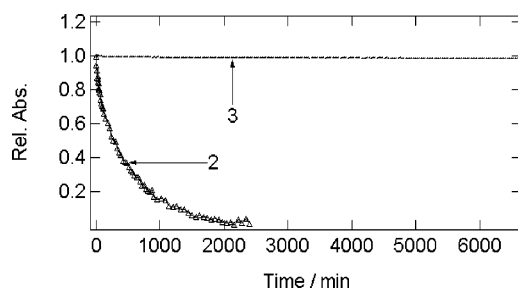


Figure 9. Thermal back reaction in the dark. Rel. Abs. is defined as $[A(t) - A_{\text{OH}}]/[A(t=0) - A_{\text{OH}}]$, with A_{OH} the absorbance of the “–OH” isomer. Absorbances measured at 500 nm for **2** and 475 nm for **3**.

Table 6. Kinetic Constants of the Thermal Back Reaction at 20 °C^a

	2 (500 nm)	3 (475 nm)
k_1/s^{-1} (A_1)	3.8×10^{-4} (0.19)	3.6×10^{-5} (0.01)
k_2/s^{-1} (A_2)	2.7×10^{-5} (0.81)	1.8×10^{-8} (0.99)
$E_a/\text{kJ mol}^{-1}$	79.0	41.2

^a The absorbance change at the absorption maximum (wavelength in parentheses) was followed and fitted by a double exponential. k_1 and k_2 are the kinetic constants with A_1 and A_2 being the relative weight of the corresponding pre-exponential factors.

ground state activation energies of the “–NH” isomer are respectively 79.0 and 41.2 kJ mol^{−1}, in the usual range of analogous compounds.^{20d,48}

Structural Change and SHG Commutation. During the recent years, X-ray structural change studies related to photochromism were reported for “P-type” (diarylethenes)⁴⁹ and “T-type” (anil,⁵⁰ bis-imidazole,⁵¹ benzylpyridine⁵²) photochromes. Such investigations are not straightforward since they involve mixtures of two different species in one single

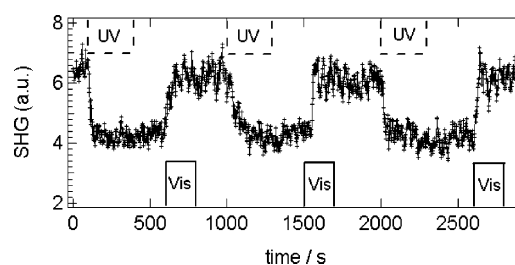


Figure 10. Photoinduced SHG switching on polycrystalline thin film of **3** (1907 nm fundamental beam).

Table 7. Light-Induced Cell Parameter Change. Data Were Recorded at 160 K

	(a) before irradiation	(b) after UV irradiation	(c) after visible irradiation
$a/\text{\AA}$	15.976(2)	15.963(4)	15.977(2)
$b/\text{\AA}$	15.977(2)	15.966(3)	15.977(2)
$c/\text{\AA}$	6.027(1)	6.020(1)	6.027(1)

crystal. In addition, “T-type” systems involve a metastable species, so molecules in the crystal are permanently in motion. Due to the exceptional thermal stability of its “–NH” form, **3** was chosen to study the influence of photochromism on structural changes. Three X-ray diffraction measurements were conducted on the same single crystal: before UV irradiation, after UV irradiation, and after a subsequent visible irradiation. X-ray patterns recorded during the first and the third experiments are exactly the same, whereas additional peaks appear for the second one, which is in fact a mixture of “–OH” and “–NH” forms.

Due to the low yield of “–OH” to “–NH” conversion, atom positions in this mixed crystal could not be obtained, and the only quantitative data we got are cell parameters (Table 7). However, we can at least conclude that the single crystalline character is preserved during the irradiation cycle and that we brought evidence of a reversible structural change, which actually occurs in the bulk.

SHG intensity (1907 nm fundamental beam) of a polycrystalline film of **3** was modified by alternate UV and visible irradiations. An SHG drop of 30% (Figure 10) was observed upon UV irradiation (3 mW cm^{−2}). This change was reversible, as it was also during a similar experiment at 1200 nm (IR nonpolarized continuum) on single crystals of **2** and **3** under a confocal microscope (see Experimental Section). In this case, the SHG decrease was respectively 10% and 40% with UV irradiation of 75 mW cm^{−2}. Although higher extents of SHG switching^{7a} (75% by photoinduced^{8a} and 100% by redox-induced^{9a} mechanisms) were already achieved in solution, the present results show that a reasonable switching extent can also be obtained in bulk materials and that practical applications can be hoped for.

It is important to mention that no absorbance change was detected in the 600–1000 nm region during these experiments. Hence, the SHG modulation can be attributed to structural and/or NLO property changes of the material during the photoinduced reaction, and not to the absorbance change. The reason for the SHG intensity drop during the evolution of the “–NH” isomer is due to either lower NLO properties of “–NH” compared to “–OH” or geometrical changes induced by the photoinduced reaction.

(48) Shen, M. Y.; Zhao, L. Z.; Goto, T.; Mordzinski, A. *J. Chem. Phys.* **2000**, *112*, 2490.

(49) (a) Kobatake, S.; Shibata, K.; Uchida, K.; Irie, M. *J. Am. Chem. Soc.* **2000**, *122*, 12135. (b) Morimoto, M.; Kobatake, S.; Irie, M. *J. Am. Chem. Soc.* **2003**, *125*, 11080 and references herein.

(50) Harada, J.; Uekusa, H.; Ohashi, Y. *J. Am. Chem. Soc.* **1999**, *121*, 5809.

(51) Kawano, M.; Sano, T.; Abe, J.; Ohashi, Y. *J. Am. Chem. Soc.* **1999**, *121*, 8106.

(52) Naumov, P.; Sekine, A.; Uekusa, H.; Ohashi, Y. *J. Am. Chem. Soc.* **2002**, *124*, 8540.

By these structural and NLO properties changes, we can assume that not only the surface but also some part of the bulk is affected by the photochemical process. Moreover, when micrometer-scale single crystals of **3** are irradiated, the absorbance of the “-NH” form increases with the thickness.

Conclusion

In summary, we succeeded in getting two compounds with suitable structures for bulk NLO properties, by forming “head-to-tail” alignment or chiral helix. Powder test SHG intensity are respectively 10 and 3 vs urea for **2** and **3**. Moreover, **3** has the most stable “-NH” isomer with a half-life of 460 days; hence, it is almost bi-stable. In these materials a rather small motion in the bulk can induce significant changes on optical properties and they match our goal to get reversible and repeatable SHG switches. Performance of the SHG switching could be even optimized in the future by using other photochromic systems having two stable forms and better conversion in solid state like diarylethenes,¹⁷ and by optimizing the penetration depth of the excitation beam in the bulk.

Such materials open a wide range of applications as optical memories or as components in optical signal processing.⁵³ Several properties of photochromic crystals are yet to be investigated. First, anisotropy in crystals can be exploited for multiplexing information within the same material.^{48,54} Second, reports on flash photolysis experiments show that

photochromic molecules switch at ps time scale, both in solution and in solid state.⁵⁵ In crystals of **3**, the “-NH” form is produced within 200 ps.⁴⁶ On a macroscopic scale, the switching speed is limited by the available photon flux vs the number of molecules that have to be switched to get noticeable property changes, and not by the reaction itself. If a small number of molecules are addressed, devices operating in the GHz to THz regimes can be targeted.

Acknowledgment. The authors thank Dr. Robert Pansu, Dr. Eléna Ishow, Mr. Jean-Jacques Vachon, Mr. Arnaud Spangenberg, and Mr. Jean-François Delouis for their help and expertise in sample preparation and measurements. They also thank Prof. Jacques A. Delaire for helpful discussions and Ms. Laure Vendier for analysis of spectral X-ray data. This work was supported by the French Ministry of Research (ACI Physico-Chimie de la Matière Complexe). The French-Japanese bilateral graduate program (Collège Doctoral Franco-Japonais), the Ecole Doctorale Physico-Chimie du Sud de Paris, and CNRS (GDR COMES and GDR POM3) sponsored this collaboration and M.S.’s stays in partner laboratories.

Supporting Information Available: X-ray crystallographic data for compounds **2** and **3** (CIF). This material is available free of charge via the Internet at <http://pubs.acs.org>. Deposited Data: CCDC 261613 and 261614.

CM050929O

(53) Kawata, S.; Kawata, Y. In ref 2d, 1777.

(54) Shibata, K.; Muto, K.; Kobatake, S.; Irie, M. *J. Phys. Chem. A* **2002**, *106*, 209.
(55) (a) Mitra, S.; Tamai, N. *Phys. Chem. Chem. Phys.* **2003**, *5*, 4647. (b) Miyasaka, H.; Nobuto, T.; Tamai, N.; Irie, M. *Chem. Phys. Lett.* **1997**, *269*, 281. (c) Suzuki, M.; Asahi, T.; Masuhara, H. *Phys. Chem. Chem. Phys.* **2002**, *4*, 185.